[CANCER RESEARCH 63, 5344–5351, September 1, 2003]

Identification of Novel Gene Expression Targets for the Ras Association Domain Family 1 (*RASSF1A*) Tumor Suppressor Gene in Non-Small Cell Lung Cancer and Neuroblastoma[1]

Angelo Agathanggelou, Ivan Bièche, Jalal Ahmed-Choudhury, Barbara Nicke, Reinhard Dammann, Shairaz Baksh, Boning Gao, John D. Minna, Julian Downward, Eamonn R. Maher, and Farida Latif[2]

Section of Medical and Molecular Genetics, Division of Reproductive and Child Health, University of Birmingham, Birmingham B15 2TT, United Kingdom [A. A., J. A-C., E. R. M., F. L.]; Laboratoire d'Oncogénétique-INSERM E0017, Centre René Huguenin, F-92210 St-Cloud, France [I. B.]; Signal Transduction Laboratory, R222, Cancer Research United Kingdom London Research Institute, London WC2A 3PX, United Kingdom [B. N., S. B., J. D.]; AG Tumorgenetik der Medizinischen Fakultät, Martin-Luther Universität Halle-Wittenberg, D-06097 Halle (Saale), Germany [R. D.]; Hamon Center for Therapeutic Oncology Research, University of Texas Southwestern Medical Center at Dallas, Texas 75390-8593 [B. G., J. D. M.]; and Cancer Research United Kingdom Renal Molecular Oncology Research Group, University of Birmingham, Birmingham B15 2TG, United Kingdom [E. R. M., F. L.]

ABSTRACT

***RASSF1A* is a recently identified 3p21.3 tumor suppressor gene. The high frequency of epigenetic inactivation of this gene in a wide range of human sporadic cancers including non-small cell lung cancer (NSCLC) and neuroblastoma suggests that *RASSF1A* inactivation is important for tumor development. Although little is known about the function of *RASSF1A*, preliminary data suggests that it may have multiple functions. To gain insight into *RASSF1A* functions in an unbiased manner, we have characterized the expression profile of a lung cancer cell line (A549) transfected with *RASSF1A*. Initially we demonstrated that transient expression of *RASSF1A* into the NSCLC cell line A549 induced G_1 cell cycle arrest, as measured by propidium iodide staining. Furthermore, annexin-V staining showed that *RASSF1A*-expressing cells had an increased sensitivity to staurosporine-induced apoptosis. We then screened a cDNA microarray containing more than 6000 probes to identify genes differentially regulated by *RASSF1A*. Sixty-six genes showed at least a 2-fold change in expression. Among these were many genes with relevance to tumorigenesis involved in transcription, cytoskeleton, signaling, cell cycle, cell adhesion, and apoptosis. For 22 genes we confirmed the microarray results by real-time RT-PCR and/or Northern blotting. *In silico*, we were able to confirm the majority of these genes in other NSCLC cell lines using published data on gene expression profiles. Furthermore, we confirmed 10 genes at the RNA level in two neuroblastoma cell lines, indicating that these *RASSF1A* target genes have relevance in non-lung cell backgrounds. Protein analysis of six genes (*ETS2, Cyclin D3, CDH2, DAPK1, TXN,* and *CTSL*) showed that the changes induced by *RASSF1A* at the RNA level correlated with changes in protein expression in both non-small cell lung cancer and neuroblastoma cell lines. Finally, we have used a transient assay to demonstrate the induction of *CDH2* and *TGM2* by *RASSF1A* in NSCLC cell lines. We have identified several novel targets for *RASSF1A* tumor suppressor gene both at the RNA and the protein levels in two different cellular backgrounds. The identified targets are involved in diverse cellular processes; this should help toward understanding mechanisms that contribute to *RASSF1A* biological activity.**

INTRODUCTION

The high incidence of loss of heterozygosity at 3p21.3 in many sporadic human cancers suggests that this locus harbors one or more critical TSGs[3] (1–6). The minimum critical interval was narrowed to ~120 kb by the discovery of overlapping homozygous deletions in lung and breast tumor cell lines (7, 8). Eight candidate TSGs were cloned from this gene-rich region including *CACNA2D2*, *PL6*, *101F6*, *NPRL2/G21*, *BLU*, *RASSF1*, *FUS1*, and *LUCA2* (9). However, conventional mutation analysis did not reveal frequent mutations in any of the above candidate genes (9–12). Nevertheless, the long isoform of *RASSF1*, *RASSF1A*, was found to be down-regulated in many lung tumor cell lines, although expression of the shorter isoform, *RASSF1C*, was unaffected (9, 13). The promoter region of *RASSF1A* is associated with a CpG island, and bisulphite DNA sequencing demonstrated that *RASSF1A* was inactivated by promoter region hypermethylation in the majority of lung tumor cell lines (13–15). This is supported by the observed reexpression of *RASSF1A* in cell lines treated with demethylating agents. Further evidence for the candidacy of *RASSF1A* as a major 3p21.3 TSG comes from *in vitro* and *in vivo* growth studies in which *RASSF1A* drastically reduced colony formation, suppressed anchorage-independent growth, and inhibited tumor formation in nude mice (13, 15). Subsequently, frequent *RASSF1A* methylation has been detected in many other tumor types, including SCLC and NSCLC; breast, kidney, prostate, and testicular cancer; neuroblastoma; phaeochromocytoma; and gastric and nasopharyngeal cancer, indicating that the inactivation of *RASSF1A* is important in the pathogenesis of many human cancers (13–22).

RASSF1A is a M_r 39,000 (340 aa) protein containing two major putative functional domains including a diacylglycerol (DAG)-binding domain (50–101 aa) at the NH_2 terminus. A *RAS* association (RA) domain (194–288 aa) in the COOH terminus (also found in the *C* isoform) suggests *RASSF1* proteins function as *RAS*-effectors (9, 23). However, recent studies indicated that it is unlikely that *RASSF1A* or *RASSF1C* bind directly to *RAS* (24). *RASSF1A* does, however, heterodimerize with the closely homologous mouse *RAS*-GTP-binding protein, *Nore1* (24–25). Human *NORE1* interacts with the proapoptotic protein kinase *MST1* to mediate a novel *RAS*-regulated apoptotic pathway (26). *RASSF1A* also interacts with *MST1*, suggesting that there might be a close interplay between *RASSF1A* and *NORE1* proteins in *RAS*-mediated apoptosis. Support for a role for *RASSF1A* in *RAS*-signaling pathways was implied by a recent study that compared the frequency of *RASSF1A* methylation with the incidence of *K-RAS* mutation in colorectal cancers (27). An inverse relationship between these events was detected in a significant number of cases.

A recent study in the NSCLC cell line NCI-H1299 suggested that *RASSF1A* might inhibit cell cycle progression (28). Thus *RASSF1A* induced G_1-S phase cell cycle arrest and blocked accumulation of *Cyclin D1*. The latter point was confirmed using siRNA to eliminate

Received 2/26/03; revised 5/30/03; accepted 6/2/03.

The costs of publication of this article were defrayed in part by the payment of page charges. This article must therefore be hereby marked *advertisement* in accordance with 18 U.S.C. Section 1734 solely to indicate this fact.

[1] Supported in part by SPARKS (Sports Aiding Medical Research for Kids), The Wellcome Trust, Cancer Research United Kingdom, and National Cancer Institute, NIH, Grants P50 CA70907 and CA71618.

[2] To whom requests for reprints should be addressed, at Section of Medical and Molecular Genetics, Department of Paediatrics and Child Health, University of Birmingham, The Medical School, Edgbaston, Birmingham B15 2TT, United Kingdom. Phone: 44-0-121-627-2741; Fax: 44-0-121-627-2618; E-mail: flatif@hgmp.mrc.ac.uk.

[3] The abbreviations used are: TSG, tumor suppressor gene; NSCLC, non-small cell lung cancer; aa, amino acid(s); siRNA, small interfering RNA; RT-PCR, reverse transcription-PCR; ECM, extracellular matrix.

endogenous *RASSF1A* from HeLa cells with the concomitant increase in *Cyclin D1* protein.

These studies suggest that *RASSF1A* may have multiple functions. To further define the possible range of functions, we have used cDNA microarray technology to investigate the global impact of *RASSF1A* on gene expression in NSCLC. In addition, we investigated the consistency of candidate *RASSF1A* target genes among NSCLC cell lines and compared the profile of *RASSF1A* target genes in NSCLC and neuroblastomas.

MATERIALS AND METHODS

Cell Culture and Transfection. The NSCLC cell lines A549 and NCI-H1299 and neuroblastoma cell lines CHP212 and SK-N-AS were obtained from American Type Culture Collection and maintained in DMEM supplemented (Invitrogen) with 10% FCS. Cells (1×10^4) were seeded and transfected with 1 μg of pcDNA3.1 or pcDNA3.1/*RASSF1A* using Fugene 6 reagent (Roche). Twenty-four h after transfection, DMEM was supplemented with 500 μg/ml Geneticin (Invitrogen). Surviving colonies were harvested and expanded in separate flasks 14 days later.

Transient transfection was set-up similarly using pEGFP-C1, pEGFP-C1/*RASSF1A*, pcDNA3/*HA-RASSF1A*, and Effectene reagent (Invitrogen). Cells were harvested using trypsin or lysis buffer (see below) 48 h after transfection.

Apoptosis Assay. Annexin-V binding was used to measure apoptosis. One $\times 10^5$ cells were seeded in 6-well dishes. Sixteen h later, DMEM was supplemented with 1 μg/ml staurosporine (Roche). Cells were incubated for 4 h and were harvested in ice-cold PBS. Cells were washed once with annexin-V binding buffer (10 mM HEPES/NaOH (pH 7.4), 140 mM NaCl, and 2.5 mM $CaCl_2$) and incubated at room temperature with 5 μl each of annexin-V-PE (Phycoethrin) and 7-AAD (7-Amino-actinomycin D) in 100 μl of binding buffer (Annexin-V-PE apoptosis detection kit; BD PharMingen) for 15 min in the dark. 400 μl of binding buffer was then added to the cells and a Coulter Epics XL-MCL flow cytometer was used to measure Annexin-V-PE binding. The assay was repeated three times.

Cell Cycle Profiling. Forty-eight h after seeding 1×10^5 cells, cells were harvested, washed with ice-cold PBS, resuspended in 70% ethanol (−20°C) and stored at −20°C for 24 h. Cells were pelleted by centrifugation, and the ethanol was decanted. Cells were stained with propidium iodide, and DNA content was analyzed by flow cytometry using a Coulter Epics XL-MCL flow cytometer running System II software. Three independent experiments were conducted.

Microarray. RNA was extracted from 50–70% confluent cells using Trizol Reagent (Invitrogen) in accordance with the manufacturer's instructions. Aliquots (25 μg) of RNA were spiked with bacterial-RNA mixture for control and was ethanol-precipitated. The RNA mix was resuspended in H_2O, was incubated for 5 min at 70°C with 5 μg of anchored oligo-dT_{17}, and was snap-chilled on ice. Cy3- or Cy5-labeled cDNA was generated by incubating the RNA/oligo-dT mix with 1× first-strand buffer [0.03 M DTT, 5 mM dNTP mix, 0.1 mM dCTP-Cy3 or dCTP-Cy5 (Amersham), and 400 units of Superscript II (Invitrogen)] for 2 h at 42°C. RNA was removed by hydrolysis in 0.05 M NaOH at 70°C for 20 min. Unincorporated nucleotides were removed using AutoSeq G-50 columns (Amersham). Cy3- and Cy5-labeled ss (single-stranded) cDNA generated from separate samples were combined with 6 μl of human cot1 DNA (1 μg/μl) and 7 μl of 3 M sodium acetate (pH 5.2) and were ethanol-precipitated. The Cy3/Cy5 ss cDNA/cot1 DNA pellet was resuspended in 8 μl of H_2O and 40 μl of hybridization buffer [5× SSC, 6× Denhardt's solution, 60 mM Tris-HCl (pH 7.6)], boiled for 5 min and cooled at room temperature for 10 min. The hybridization mix was then applied to precooled (4°C) Hver1.2.1 cDNA microarrays [Microarray consortium (MACS)], was overlaid with a coverslip and incubated at 47°C for 12–24 h in a humidified atmosphere. Microarrays were washed sequentially with 2× SSC, 0.1× SSC/0.1% SDS, and 0.1× SSC and were air-dried by briefly spinning in a centrifuge to remove excess liquid. The relative binding of Cy3- and Cy5-labeled ss cDNA was measured using a LSI-Lumonics SA4000 scanner and GeneSpring Expression Analysis Software (Silicon Genetics) was used to analyze the data.

Real-Time RT-PCR. Quantitative values are obtained from the cycle number (*Ct* value) at which the increase in fluorescent signal associated with an exponential growth of PCR products starts to be detected by the laser detector of the ABI Prism 7700 Sequence Detection System (Perkin-Elmer Applied Biosystems, Foster City, CA) using the Perkin-Elmer Biosystems analysis software according to the manufacturer's manuals.

The precise amount of total RNA added to each reaction mix (based on absorbance) and its quality (*i.e.*, lack of extensive degradation) are both difficult to assess. We, therefore, also quantified transcripts of the *TBP* gene coding for the TATA box-binding protein (a component of the DNA-binding protein complex TFIID) as the endogenous RNA control, and each sample was normalized on the basis of its *TBP* content.

Results, expressed as *N*-fold differences in target gene expression relative to the *TBP* gene, termed "N_{target}," were determined by the formula: $N_{target} = 2^{\Delta Ctsample}$, where ΔCt value of the sample was determined by subtracting the average *Ct* value of the target gene from the average *Ct* value of the *TBP* gene.

The N_{target} values of the samples were subsequently normalized so that the mean of the N_{target} values of the *RASSF1A*-null-transfected samples of each cell line would equal a value of 1.

Primers for the *TBP* and *RASSF1A* and the 15 target genes were chosen with the assistance of the computer programs Oligo 5.0 (National Biosciences, Plymouth, MN). To avoid amplification of contaminating genomic DNA, one of the two primers was placed, if possible, in a different exon. In general, amplicons were between 70 and 120 nucleotides. Agarose gel electrophoresis allowed us to verify the specificity of PCR amplicons.

Total RNA extracted from cell line samples was reverse-transcribed before real-time PCR amplification. PCR was performed using the SYBR Green PCR Core Reagents kit (Perkin-Elmer Applied Biosystems). The thermal cycling conditions included an initial denaturation step at 95°C for 10 min and 50 cycles at 95°C for 15 s and 65°C for 1 min. Experiments were performed with duplicates for each data point.

Northern Blotting. RNA (20 μg) was separated on standard agarose–formaldehyde gel at 100 V for 3 h. RNA was transferred by capillary blotting overnight onto Hybond N+ membrane (Amersham-Pharmacia Biotech) in Northern transfer buffer (Sigma). RNA was fixed onto the membrane by baking at 80°C for 2 h. Gene fragments (typically 500–700 bp) for use in probe synthesis were excised by restriction enzyme digestion from cDNA clones (Sanger Centre). cDNA probes were labeled with α-^{32}P (Amersham) using a random priming kit (Roche) in accordance with the manufacturer's instructions. The probes were purified from unincorporated nucleotides on Sephadex 50 columns (Roche) and denatured. Hybridization was performed overnight at 68°C in PerfectHyb Plus hybridization buffer (Sigma). Membranes were washed according to manufacturer's instructions, exposed with phosphorimager cassettes, and analyzed on phosphorimager program ImageQuant (Molecular Dynamics).

Western Blotting and Immunofluorescence. Cells were grown to ~70% confluence and harvested in NP40-lysis buffer. Lysates were incubated on ice for 10 min, and sonicated for 60 s, and insoluble cell debris was removed by centrifugation for 5 min at 14,000 rpm at 4°C. Protein samples (20 μg each) were separated by SDS-PAGE (6–15%) and were electroblotted to Hybond-P membranes (Amersham Biosciences). Immobilized proteins were detected using appropriate primary and horseradish-peroxidase secondary antibodies by ECL (Amersham Bioscience).

For immunofluorescence detection of *CDH2*, cells were seeded onto Superfrost glass slides (VWR International) 24 h before fixing in acetone for 15 min. All of the antibody incubations and washes were done with PBS. Immobilized anti-*CDH2* was detected using Cy3-labeled rabbit antimouse (Sigma). Cells were counterstained and mounted using 4′,6-diamidino-2-phenylindole (DAPI)/Vector mount.

Antibodies. Anti-*RASSF1A* monoclonal antibody (eB114) was purchased from eBiosciences; anti-*ETS2* (C-20) was purchased from Santa Cruz Biotechnology; anti-*Pro-cathepsin L* (Ab-2) and anti-*TGM2* (rabbit) were purchased from Calbiochem; anti-*Thioredoxin* was purchased from Serotec; anti-HA (HA-7), anti-*DAPK1*, and anti-*CDH2*/*A-CAM* (GC-4) were purchased from Sigma, anti-*CCND3* (DCS22) was purchased from the monoclonal antibody service, Cancer Research United Kingdom; and anti-*Cyclin D1* was kindly provided by G. Peters, Cancer Research UK (formerly, ICRF), London, United Kingdom.

RESULTS

Characterization of A549 Clones Stably Expressing *RASSF1A*

Transfection of *RASSF1A* into A549 Cells Induces G_1 Cell Cycle Arrest and Down-Regulates Cyclin D1 Expression. We used propidium iodide incorporation to investigate the effect of *RASSF1A* on cell cycle progression in the NSCLC cell line A549 (Fig. 1*A*). *RASSF1A* expression resulted in an increase of cells in the G_1 phase of the cell cycle 48 h after transfection compared with GFP-expressing cells [Fig. 1*A*(*i*)].

To determine whether the G_1-arrested phenotype was maintained after drug selection, stably transfected clones of A549 were then analyzed. Expression of *RASSF1A* was confirmed by RT-PCR (data not shown) and by Western blotting (Fig. 1*B*). A representative clone expressing *RASSF1A* (Cl.5) was found to have an increased cell population in the G_1 phase of the cell cycle compared with the vector control clone (V18), indicating that the cell cycle effect observed in transient transfection is perpetuated after drug selection [Fig. 1*A*(*ii*)].

The effect of *RASSF1A* on cell cycle may be associated with a decrease in *Cyclin D1* expression. Therefore we screened whole cell lysates from *RASSF1A* expressing clones by Western blotting to determine whether *Cyclin D1* is down-regulated in A549. *Cyclin D1* protein expression was drastically reduced in *RASSF1A*-expressing clones compared with vector controls; similar results were obtained in the neuroblastoma cell line CHP212 (Fig. 1*B*). These results indicate that the *RASSF1A* affects cell cycle progression and reduces *Cyclin D1* expression in A549 cells.

RASSF1A Increases Sensitivity to Staurosporine-induced Apoptosis. *RASSF1A* may function as a mediator of apoptosis. Hence, *RASSF1A*-expressing cells may be more sensitive to apoptotic stimuli. We used annexin-V binding to measure the apoptosis of *RASSF1A*-expressing A549 cell derivatives incubated with staurosporine. *RASSF1A*-expressing cells showed a 29.1% increase in apoptosis relative to control cells after treatment with staurosporine (Fig. 1*C*).

Genes Differentially Regulated by *RASSF1A*. To determine changes in gene expression that result from the reintroduction of *RASSF1A* into A549, we have used a competitive hybridization-based approach to screen Hver1.2.1 cDNA microarrays containing ~6000 unique genes (does not include *Cyclin D1*). RNA was extracted from duplicate cultures of representative derivatives of A549 (*RASSF1A*-expressor Cl.5 and vector-control V.18). To reduce variations in gene expression caused by culture conditions, we harvested RNA from cells at 60–70% confluency, and 48 h after seeding, we generated cDNA labeled with Cy3 and Cy5 from each sample. Competitive hybridizations were done in duplicate using Cy3- and Cy5-labeled cDNA from each preparation. Furthermore, Cy3- and Cy5-labeled cDNA from each of the vector samples was used in duplicate control hybridizations to eliminate background noise caused by possible differences in labeling efficiency of the Cy dyes and variable genes. In total, eight Hver1.2.1 chips were screened: four *RASSF1A versus* vector and four control hybridizations. Data were analyzed using GeneSpring software. Essentially the GeneSpring software passed data sets that showed a significant increase or decrease. From these, data sets that showed significant changes in the control hybridizations were filtered. Stringency was set so that only the data sets with a minimum 2-fold change and agreement in four of four *RASSF1A versus* vector hybridizations were passed. Table 1 lists 66 genes arranged into functional groups derived from 74 data sets that have met the set criteria. Of the 66 genes differentially expressed in response to *RASSF1A*, 34 were induced, whereas 32 were down-regulated.

Northern and Quantitative Real-Time RT-PCR Confirmation of Microarray Data

Six of the identified *RASSF1A* targets were selected for confirmation by Northern blotting in the same clones used for microarray analysis (Fig. 2). Quantification revealed a good correlation between the fold changes obtained in the microarray and Northern blotting for *DUSP1*, *CA12*, *HPCAL1*, *ABCG2*, *SM22*, and *CTSB*.

Quantitative real-time RT-PCR was used to investigate the expression levels of 17 target genes in three *RASSF1A*-expressing clones of A549. The data obtained is presented in Table 2. There was complete correlation between the real-time RT-PCR results and the microarray data for all of the A549 clones analyzed. This included 6 induced genes (*ZYX*, *CDH2*, *TPM1*, *ETS2*, *ANPEP*, and *SPARC*) and 11 down-regulated genes (*ITGB5*, *PIGPC1*, *ATP5H*, *DB1*, *DAPK1*, *CCND3*, *TXN*, *CTSL*, *EDG2*, *SPINT2*, and *CA12*). This confirmed the microarray data and demonstrated that *RASSF1A* has a reproducible

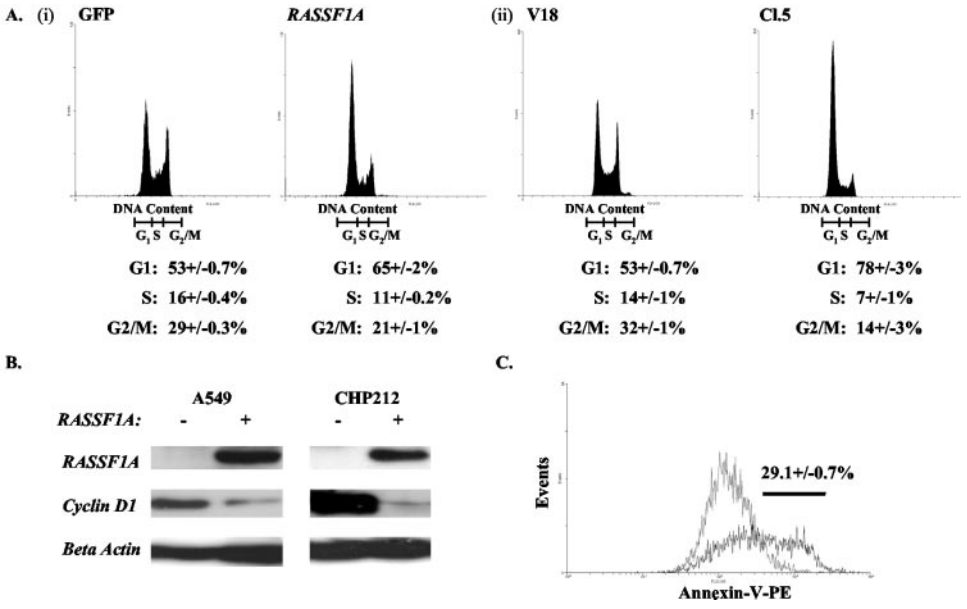

Fig. 1. *A*, cell cycle profiles of A549 cells transiently and stably expressing *RASSF1A*. (*i*), A549 cells transfected with GFP or RASSF1A-GFP were harvested and analyzed after 48 h incubation. (*ii*), representative clones of A549 (V.18 and Cl.5) were harvested for analysis 48 h after seeding. Cells were stained with propidium iodide, and the percentage in G_1, S phase and G_2-M was determined by fluorescence-activated cell sorting (FACS) analysis ($n = 3$). *B*, total cell lysates of A549 and CHP212 derivatives were subjected to polyacrylamide (15%) gel electrophoresis and analyzed for expression of the specified proteins by Western blotting. Blots were stripped and reprobed with a β-actin antibody to demonstrate protein loading. *C*, flow-cytometric analysis of annexin-V-PE binding in A549-V control (*gray line*) and A549-*RASSF1A* (*black line*) cells treated with 1 μg/ml staurosporine for 4 h ($n = 3$).

Table 1 *Genes differentially expressed by RASSF1A in NSCLC cell line A549*

GenBank accession no.	Unigene cluster identification	Common name	Average fold change[a]	Description
Transcription				
U24576	Hs.3844	*LMO4*	2.2	Lim domain only 4
AF017257	Hs.85146	*ETS-2*	2.2	Virus oncogene homolog 2 protein (*ets-2*) gene
U31913	Hs.75305	*AIP*	0.4	Aryl hydrocarbon receptor-interacting protein
NM_015842	Hs.5978	*LMO7*	0.5	LIM domain only 7
AB007836	Hs.25511	*TGFB1/1*	3.1	Transforming growth factor β 1 induced transcript 1
Signaling/Proliferation				
AA099910	Hs.291	*ENPEP*	2.3	Glutamyl aminopeptidase
N94424	Hs.82547	*RARRES1*	3.7	RARRES1 retinoic acid receptor responder 1
D43639	Hs.394	*AM*	2.5	Adrenomedullin
U80811	Hs.75794	*EDG2*	0.5	Endothelial differentiation gene 2
J04026	Hs.432922	*TXN*	0.4	Thioredoxin
X68277	Hs.171695	*DUSP1*	3.0	Dual specificity phosphatase 1
U77914	Hs.91143	*JAG1*	2.8	Ligand in NOTCH signaling pathway
S75725	Hs.119206	*IGFBP7*	3.8	Insulin-like growth factor binding protein 7
U31449	Hs.11881	*TM4SF4*	3.2	Transmembrane 4 superfamily, member 4
U79458	Hs.231840	*WBP2*	0.5	WW domain binding protein 2
AF027205	Hs.31439	*SPINT2*	0.5	Serine protease inhibitor, Kunitz-type, 2
U76702	Hs.25348	*FSTL3*	2.3	Follistatin-like 3
M19154	Hs.169300	*TGFB2*	2.1	Transforming growth factor-β2
AA228119	Hs.239138	*PBEF*	0.5	pre-B-cell colony-enhancing factor
L33930	Hs.286124	*CD24A*	3.2	CD24 signal transducer
NM_002193	Hs.1735	*INHBB*	0.4	Inhibin, βB
X60201	Hs.56023	*BDNF*	3.0	Brain-derived neurotrophic factor
AF009227	Hs.172816	*NRG1*	2.5	Neuregulin 1
U61849	Hs.84154	*NPTX1*	6.8	Human neuronal pentraxin 1
NM_020548	Hs.78888	*DBI*	0.5	Diazepam binding inhibitor
R87460	Hs.108080	*CSRP1*	2.3	Cysteine-rich protein 1
Protein synthesis/degradation				
NM_014294	Hs.4147	*TRAM*	3.0	Translocating chain-associating membrane protein
H11775	Hs.8265	*TGM2*	4.6	Transglutaminase 2
R41770	Hs.78056	*CTSL*	0.3	Pro-cathepsin L
NM_004681	Hs.155103	*EIF1AY*	2.5	Eukaryotic translation initiation factor 1A, Y chromosome
D29012	Hs.77060	*PSMB6*	0.5	Proteasome (prosome, macropain) subunit, β type, 6
NM_001908	Hs.297939	*CTSB*	2.0	Cathepsin B
NM_000475	Hs.268490	*NR0B1*	0.3	Nuclear receptor subfamily 0, group B, member 1
AF053233	Hs.172684	*VAMP8*	0.5	Vesicle-associated membrane protein 8
Contraction/calcium				
NP_002464	Hs.146550	*MYH9*	2.1	Myosin, heavy polypeptide 9, non-muscle
NM_005980	Hs.2962	*S100P*	0.3	S100 calcium-binding protein P
Metabolism				
AA463510	Hs.64	*SDHB*	5.2	SDHB succinate dehydrogenase complex, subunit B
M77693	Hs.28491	*SSAT*	0.5	Spermidine/spermine *N*1-acetyltransferase
U43944	Hs.14732	*ME1*	0.5	Cytosolic NADP(+)-dependent malic enzyme 1
NM_006356	Hs.64593	*ATP5H*	0.5	Homo sapiens ATP synthase, H+ transporting
NM_001218	Hs.5338	*CA12*	0.3	Carbonic anhydrase XII
AB032261	Hs.119597	*SCD*	0.4	Stearoyl-CoA desaturase 1
Cytoskeletal/Cell adhesion				
AA011024	Hs.378774	*ACTG2*	2.1	Actin γ2, smooth muscle, enteric
NM_014000	Hs.75350	*VCL*	2.1	Vinculin
X94991	Hs.75873	*ZYX*	2.5	Zyxin
J05633	Hs.149846	*ITGB5*	0.5	Integrin β5 subunit
M95787	Hs.75777	*SM22*	9.3	Transgelin
M19713	Hs.77899	*TPM1*	3.6	Skeletal muscle alpha-tropomyosin
M34064	Hs.161	*CDH2*	2.4	N-cadherin
ECM				
H99607	Hs.111779	*SPARC*	5.3	Secreted protein, acidic, cysteine-rich (osteonectin)
M59040	Hs.169610	*CD44*	2.0	Hyaluronic acid receptor
NM_001150	Hs.1239	*ANPEP*	2.1	Alanyl (membrane) aminopeptidase
L06139	Hs.89640	*TEK*	0.5	Receptor protein-tyrosine kinase
Cell cycle				
M90814	Hs.83173	*CCND3*	0.4	Cyclin D3
Apoptosis				
NM_004938	Hs.153924	*DAPK1*	0.5	Death-associated protein kinase 1
X86809	Hs.194673	*PEA15*	2.4	Phosphoprotein enriched in astrocytes, M_r 15,000
Others				
M90656	Hs.151393	*GCS*	0.4	γ-glutamylcysteine synthetase
AK002040	Hs.194720	*ABCG2*	0.3	ATP-binding cassette, sub-family G (WHITE), member 2
U77970	Hs.321164	*NPAS2*	0.4	Neuronal PAS2
D49387	Hs.114670	*LTB4DH*	0.4	Leukotriene b4 12-hydroxydehydrogenase
AL512758	Hs.193235	*DKFZp547D155*	0.4	Hypothetical protein DKFZp547D155
H59861	Hs.2030	*THBD*	2.3	Thrombomodulin
AF085356	Hs.246112	*KIAA0788*	0.5	U5 snRNP-specific protein, M_r 200,000
AF070616	Hs.3618	*HPCAL1*	0.5	Hippocalcin-like 1
AA135596	Hs.79516	*BASP1*	0.5	Brain-abundant signal protein, membrane-attached, 1
AJ251830	Hs.303125	*PIGPC1*	0.5	P53-induced protein

[a] Microarray data obtained using A549 clones V18 (control) and C5 (*RASSF1A*).

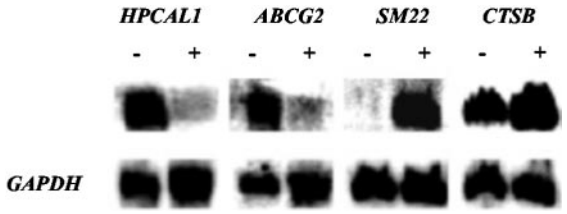

Fig. 2. Northern blot analysis showing the change in RNA expression of the indicated genes in *RASSF1A* expressing Cl.5 (+) and vector control V18 (−) A549 cells. Blots were stripped and reprobed for *GAPDH* as control for RNA loading.

Table 2 *Real-time RT-PCR showing fold change of target gene expression in A549 cells*[a]

	A549		
Gene	C1	C3	C5
ZYX	1.21	2.92	3.45
CDH2	22.94	36.89	8.78
ITGB5	0.26	0.44	0.80
PIGPC1	0.00	0.00	0.29
ATP5H	0.90	0.73	0.52
DBI	0.94	0.65	0.82
DAPK1	0.02	0.03	0.39
CCND3	0.22	0.22	0.49
TXN	0.15	0.23	0.47
CTSL	0.07	0.24	0.46
CA12	0.00	0.03	0.17
SPARC	32367	331180	13468
TPM1	2.95	6.39	4.87
ETS2	2.55	3.15	5.05
ANPEP	3.73	1.19	17.94
EDG2	0.45	0.13	0.39
SPINT2	0.00	0.00	0.34

[a] Data expressed as fold change relative to vector control clone V18 (0.00 = <0.01).

effect on the expression of these genes in A549. For control, two separate primer sets were used to quantify *RASSF1A* expression.

In Silico Comparison of Target Gene Expression in *RASSF1A*-expressing A549 *versus* Other NSCLC Cell Lines of Known *RASSF1A* Status

We wished to determine to what extent the genetic background of individual cell lines might influence the expression profile of candidate *RASSF1A* target genes. Expression data from microarray experiments is made available on websites such as UCSC (University of California Santa Cruz) human genome project (http://genome-archive.cse.ucsc.edu/). Ross *et al.* (29) have investigated the variation in gene expression of a wide range of human tumor cell lines including NSCLC. The *RASSF1A* expression status of four of the NSCLC cell lines used (A549, NCI-H460, NCI-H332, and NCI-H23) is known. The *RASSF1A* promoter region in these cell lines is methylated and *RASSF1A* is not expressed. This information provided us with an opportunity to compare target gene expression in our A549 derivatives with the levels of target genes in this panel of NSCLC cell lines determined by Ross *et al.* (Fig. 3). The inclusion of A549 in the Ross study is a useful control. Expression data were available for 17 of 22 confirmed *RASSF1A* gene targets. Overall, the expression of the target genes in the NSCLC cell panel (not expressing *RASSF1A*), with the exception of *DAPK1*, was the opposite of that observed in *RASSF1A*-expressing A549 cells indicating that these genes are *RASSF1A* regulated. In the Ross data, *TPM1* appears to be up-regulated in A549, whereas it seems to be down-regulated in the other NSCLC cell lines. Closer inspection of the Ross data shows that *TPM1* is up-regulated 2-fold in A549, whereas we show a 5-fold increase in *RASSF1A*-expressing A549 cells. These differences are likely to be attributable to the differences in reference RNA used in each study.

Analysis of *RASSF1A* Target Genes in Neuroblastoma Cell Lines

Having established that the profile of *RASSF1A* candidate target genes was similar between different NSCLC cell lines *in silico*, we wished to determine whether *RASSF1A* targets in NSCLC were also regulated in neuroblastoma cell lines. Real-time RT-PCR confirmation of the microarray data were extended to include *RASSF1A* expressing clones of two neuroblastoma cell lines SK-N-AS and CHP212. The expression data from the SK-N-AS and CHP212 cells corroborated the results obtained in the lung background for 10 of 17 genes (*CDH2*, *TPM1*, *ETS2*, *ANPEP*, *PIGPC1*, *DB1*, *CCND3*, *TXN*, *CTSL*, and *CA12*; Table 3; Fig. 4). This shows that the majority of the

Table 3 *Real-time RT-PCR data showing the fold change of target gene expression in neuroblastoma cell lines*[a]

	CHP212			SK-N-AS	
Gene	C1	C3	C4	C2	C6
ZYX	0.09	0.12	0.08	1.05	1.09
CDH2	1.67	1.24	1.31	1.61	2.10
ITGB5	0.17	0.60	0.82	2.32	2.23
PIGPC1	0.00	0.00	0.00	0.02	0.42
ATP5H	0.68	0.64	0.58	1.21	1.28
DBI	0.32	0.40	0.35	0.85	0.74
DAPK1	1.77	1.75	1.77	2.34	2.25
CCND3	0.54	0.67	0.61	0.28	0.24
TXN	0.23	0.24	0.22	0.21	0.64
CTSL	0.31	0.32	0.29	0.83	0.72
CA12	0.28	0.06	0.07	0.27	0.65
SPARC	0.17	0.12	0.15	1.22	1.73
TPM1	3.46	2.20	1.98	2.49	2.38
ETS2	1.68	1.46	1.72	1.44	1.56
ANPEP	0.30	0.16	0.03	1.86	2.30
EDG2	2.8	1.65	2.61	0.37	0.37
SPINT2	0.17	0.58	0.69	7.69	10.39

[a] Data expressed as fold change relative to vector control clones CHP212-V1 and SK-N-AS-V1 (0.00 = <0.01).

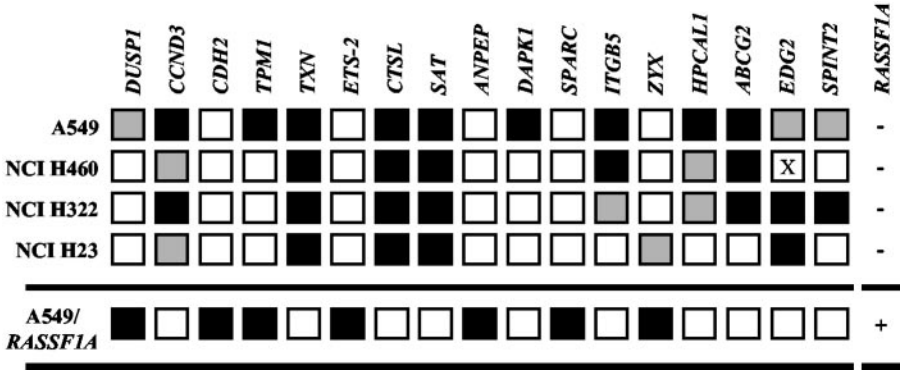

Fig. 3. *In silico* comparison of target gene expression in *RASSF1A*-expressing A549 and other NSCLC cell lines of known *RASSF1A* expression status (*shown on the right*: −, not expressed; +, expressed). The expression levels of 17 *RASSF1A* gene targets determined by Ross *et al.* (29) are indicated by *shaded boxes* (*black*, up-regulated; *white*, down-regulated; *gray*, no change; *X*, not done). The effect of *RASSF1A* on target gene expression in transfected A549 cells is shown *between the black horizontal lines*.

RASSF1A expression targets identified in A549 have relevance in the neuroblastoma background. The expression of seven genes, *SPINT2*, *EDG2*, *ITGB5*, *SPARC*, *ZYX*, *DAPK1*, and *ATP5H*, was either unaffected by *RASSF1A* in one of the two neuroblastoma cell lines (*ZYX*, *SPARC*, and *ATP5H*), or changed contrary to the effect observed in lung cancer (*DAPK1* and *ZYX*), or agreed with the results seen in lung cancer but only in one of the neuroblastoma backgrounds (*SPINT2*, *EDG2*, *ITGB5*, and *SPARC*). This raises the possibility that *RASSF1A* may also have tissue-specific effects.

Protein Confirmation of Microarray Data

To establish whether *RASSF1A*-induced effects seen at the RNA level translated to changes in protein levels, we examined the expression of *ETS2*, *CTSL*, *TXN*, *DAPK1*, *CDH2*, and *CCND3* in lung and neuroblastoma backgrounds using a combination of Western blotting and immunofluorescence. Protein levels of *CTSL*, *TXN*, and *CCND3* were greatly reduced in *RASSF1A*-expressing cells of A549 and CHP212 in agreement with changes seen at the RNA level (Fig. 5). *DAPK1*, also, was drastically down-regulated in stably transfected A549 cells. Induction of *ETS2* and *CDH2* by *RASSF1A* was confirmed by immunoblotting in both lung and neuroblastoma lineages. The change of target gene expression seen by Western blotting correlated with the level of RASSF1A protein expression in these clones. The induction of *CDH2* was further corroborated at the cellular level by immunofluorescence staining (Fig. 6).

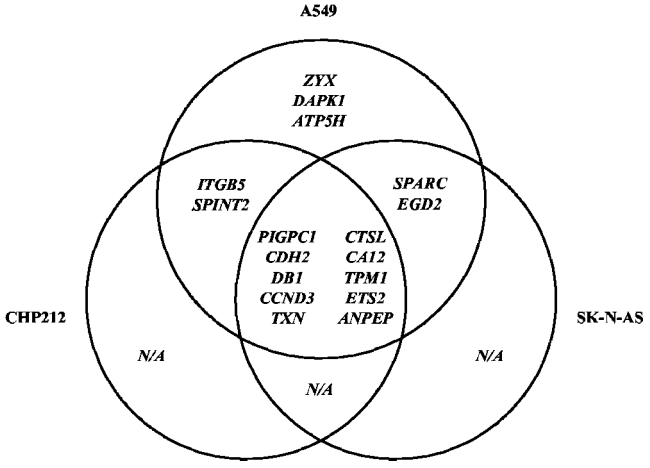

Fig. 4. Venn diagram showing the cell line distribution of *RASSF1A*-regulated genes.

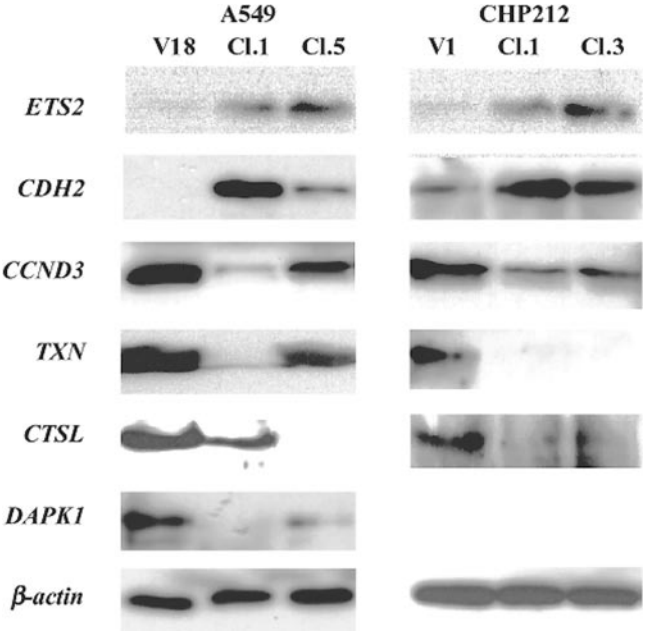

Fig. 5. Western blot analysis showing protein level changes of *RASSF1A*-regulated genes. Protein lysates from control clones (A549 V18 and CHP212 V1) and independent *RASSF1A*-expressing clones (A549 Cl.1, Cl.5 and CHP212 Cl.1, Cl.3) were separated on polyacrylamide gels and were analyzed for the indicated proteins. Antibody against *β-actin* was used to control for protein loading.

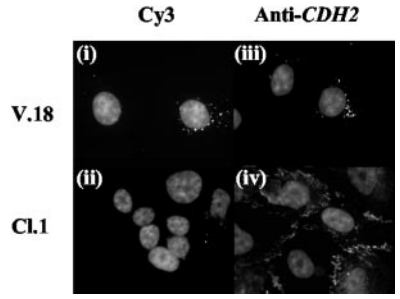

Fig. 6. Immunofluorescence staining showing induction of *CDH2* in *RASSF1A*-expressing A549 cells. (*i*) and (*ii*), negative control stains of A549-vector control (V.18) cells and the *RASSF1A*-expressing clone Cl.1, respectively. (*iii*) and (*iv*), *CDH2* staining in A549 V.18 and Cl.1, respectively. Cells were grown on glass slides, fixed with acetone and probed with mouse anti-*CDH2* (A-CAM; Sigma). Antibody binding was visualized with Cy3-labeled rabbit antimouse.

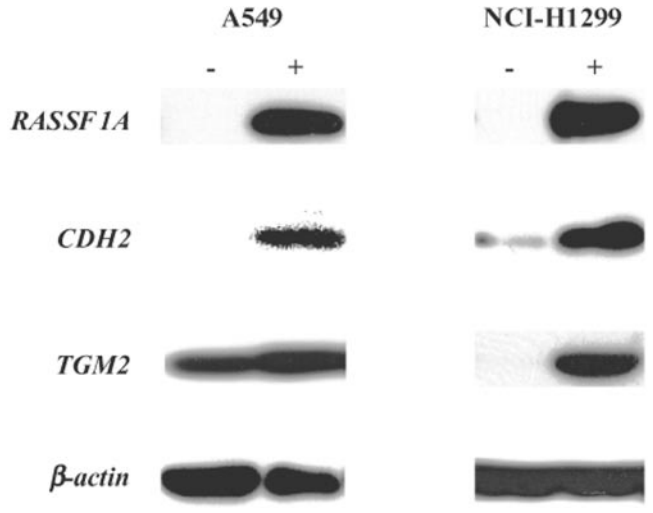

Fig. 7. Immunoblot detection of *RASSF1A*-induced expression of *CDH2* and *TGM2*. A549 and NCI-H1299 cells were transfected with pcDNA3*HA* (−) or pcDNA3*HA-RASSF1A* (+) and were harvested in lysis buffer 48 h after transfection. Proteins were resolved by PAGE and were probed for expression of the indicated proteins.

Regulation of *RASSF1A* Target Genes in Transient Assay

To further confirm the candidacy of the identified targets as *RASSF1A*-regulated genes, we set up a transient transfection assay. Fig. 7 shows that both *CDH2* and *TGM2* are strongly induced 48 h after transfection with *RASSF1A* in both A549 and NCI-H1299 cell lines, in agreement with our findings in stable clones. This effect was reproducible ($n = 2$) and also suggests that the targets identified in A549 are relevant in other NSCLC cell lines.

DISCUSSION

RASSF1A is a major 3p21.3 TSG with a high incidence of epigenetic inactivation in many common sporadic human cancers. Exogenous overexpression of *RASSF1A* has a profound effect on tumor cell

growth *in vitro* and *in vivo*; however, the mechanisms of *RASSF1A* tumor suppression are not yet understood. We have demonstrated that *RASSF1A*-induced cell cycle arrest in NSCLC A549 cells is consistent with findings in NSCLC NCI-H1299 (28). Furthermore, we show that stable exogenous overexpression of *RASSF1A* sensitized A549 cells to staurosporine-induced apoptosis. Subsequently, we used cDNA microarrays to gain insight into possible functions of *RASSF1A*. Thus, we identified 66 genes differentially up- or down-regulated by *RASSF1A* by at least 2-fold in the NSCLC cell line A549. We confirmed the changes in RNA expression by Northern blotting and or quantitative real-time RT-PCR of 22 genes. Human tumorigenesis is a multistep process, and *RASSF1A*-induced changes in gene expression might be influenced by the genetic and epigenetic background of the cell line (and the tumor type). To determine whether *RASSF1A* target gene analysis in a range of NSCLC cell lines would be consistent with that obtained in A549, we correlated the changes in candidate target gene expression in four NSCLC cell lines analyzed by Ross *et al.* (29) using microarrays. Remarkably the expression pattern of 16 of 17 target genes were confirmed by *in silico* analysis using the data deposited by Ross *et al.* Having obtained consistent results within a single tumor type, we then compared target gene expression in NSCLC and neuroblastoma cell lines. Ten genes were confirmed in two neuroblastoma cell lines (CHP212 and SK-N-AS) including *CDH2*, *TPM1*, *ETS2*, *ANPEP*, *PIGPC1*, *DB1*, *CCND3*, *TXN*, *CTSL*, and *CA12*, which indicated that these *RASSF1A* targets are common in lung and neuroblastoma cell lineages. Western analysis of six of these genes, *ETS2*, *CTSL*, *TXN*, *DAPK1*, *CDH2*, and *CCND3*, demonstrated that changes in RNA levels were paralleled by changes in protein expression in both cell backgrounds. Furthermore, *RASSF1A*-induced expression of *CDH2* was demonstrated by immunofluorescence. Interestingly, there seemed to be a correlation between the change in target gene expression and *RASSF1A* expression at the protein level in A549 cells. Transient transfection in A549 and NCI-H1299 was used to further confirm the role of *RASSF1A* in regulating the expression of target genes *CDH2* and *TGM2*. This highlights the importance of *RASSF1A* in the regulation of these genes and indicates that the targets identified in A549 are also important in other NSCLC cell lines. Our analysis of *RASSF1A* target genes in NSCLC and neuroblastoma suggests that *RASSF1A* has pleiotropic effects on tumor cell biology affecting several pathways important in tumorigenesis, including cell cycle progression, cell adhesion, cell migration, angiogenesis, transcription, and apoptosis.

Our data suggests that regulation of the cell cycle may be just one mechanism through which *RASSF1A* regulates cell proliferation. Exogenous overexpression of *RASSF1A* inhibited cell cycle progression, which was consistent with the observed down-regulation of *Cyclin D1* and *D3* protein levels. In addition, we found that *RASSF1A* affects the expression of genes involved in the regulation of cell growth such as *Diazepam binding inhibitor* (*DBI*) and *Spermidine/spermine N1-acetyltransferase* (*SSAT*). At this stage, it is not possible to determine whether the effect of *RASSF1A* on the cell cycle and the observed down-regulation of cyclins is a direct effect or a downstream effect of altered expression of genes that regulate cell growth.

Cell-cell adhesion and cell-substratum adhesion are thought to affect cell migration, proliferation, and apoptosis. Through proteins such as *N-cadherin* (*CDH2*), *Zyxin* (*ZYX*) and *Tropomyosin1* (*TPM1*), *RASSF1A* may influence these cellular functions, which ultimately affect cell behavior. Loss of expression of *CDH2*, *ZYX*, and *TPM1* has been linked with cell transformation, gain of contact-independent growth, and development of metastasis (30–35). *RASSF1A*-expressing cells have reduced contact-independent growth and form fewer metastases in nude mouse assays. Hence, it is tempting to speculate that *RASSF1A*-induced expressing of *CDH2, ZYX,* and *TMP1* may contribute to this phenotype.

A characteristic of many tumors is the ability to change and reshape the ECM especially during angiogenesis and migration. Our data suggests that *RASSF1A* plays a role in regulating these processes by down-regulating *Cathepsin L* (*CTSL*) and increasing the expression of *SPARC* (*Secreted protein acidic and rich in cysteine/Osteonectin*). *CTSL* is a cysteine proteinase that is active against substrates such as *elastin*, *collagen*, *actin laminin*, and *fibronectin* (36). In neoplasia, *CTSL* promotes tumor cell invasion and metastasis (37). *SPARC* is a multifunctional matricellular protein. Among its reported effects are the inhibition of breast tumor cell line proliferation and the inhibition of growth and angiogenesis in neuroblastoma (38, 39).

Modulation of target gene expression can be achieved in different ways, including at the level of transcription. *RASSF1A* affects the expression of some transcriptional regulators, including *ETS-2,* that belong to the *ETS* family of transcription factors, which are important downstream targets of the *RAS/RAF/MEK/MAPK*-signaling pathway (40). Phosphorylation of specific residues in *ETS-2* by *MAP-kinase* is essential for *RAS*-mediated *ETS-2* activation. However, whereas *ETS-2* activation by *RAS* is important during transformation, increased expression of *ETS-2* has been shown to reverse *RAS*-mediated transformation (41). At this stage, it is not clear which of the *RASSF1A*-induced changes in gene expression are attributable to the secondary effects of alterations in transcription factor levels.

Resistance to apoptosis is an important part of tumorigenesis. *RASSFIA* is suggested to be a mediator of *RAS*-induced apoptosis. Consistent with this, we showed that *RASSF1A* sensitized cells to staurosporine-induced apoptosis. However, our results suggest that *RASSF1A* down-regulates the expression of *Death-associated protein kinase1* (*DAPK1*) in stable clones of A549 cells but not in neuroblastoma cell lines, which showed increased expression by real time RT-PCR. This variance still needs to be resolved. It has been shown that promoter methylation has a role in inactivating *DAPK1* in some cancers. However, recent studies show that *DAPK1* is unmethylated in A549 cells, suggesting that its unresponsiveness is unlikely to be caused by promoter methylation (42). Interestingly, we show that *RASSF1A* strongly induced the expression of *Transglutaminase 2* (*TGM2*), which is also involved in apoptosis (reviewed in 43). *TGM2* functions both as a calcium-dependent transglutaminase and as a G-protein (G_h) modulating phospholipase activity (44) and also has roles in bone ossification, wound healing (45), cell adhesion (46), and cell signaling (47). This suggests that through *TGM2, RASSF1A* may not only affect apoptosis but several other important cellular functions.

Some of the *RASSF1A* expression targets such as *CTSL* and *TPM1* are also modulated by the oncogene *RAS* during transformation (35, 38, 41, 48). Regulation of such genes implies that one of the functions of *RASSF1A* may be to regulate the expression of *RAS* gene targets. How this is achieved needs further investigation. However, it is interesting to note that *DUPS1*, a regulator of *MAP-kinase* activity, and *ETS-2* are among the list of *RASSF1A* gene targets.

Overall, our global approach to characterizing the role of *RASSF1A* raises the possibility that it functions as a regulator of a number of key processes important for tumor progression, which supports its status as a major 3p21.3 TSG.

REFERENCES

1. Wistuba, I. I., Behrens, C., Virmani, A. K., Mele, G., Milchgrub, S., Girard, L., Fondon, J. W., III, Garner, H. R., McKay, B., Latif, F., Lerman, M. I., Lam, S., Gazdar, A. F., and Minna, J. D. High resolution chromosome 3p allelotyping of human lung cancer and preneoplastic/preinvasive bronchial epithelium reveals multiple, discontinuous sites of 3p allele loss and three regions of frequent breakpoints. Cancer Res., *60:* 1949–1960, 2000.

2. Martinez, A., Fullwood, P., Kondo, K., Kishida, T., Yao, M., Maher, E. R., and Latif, F. Role of chromosome 3p12-*p21* tumour suppressor genes in clear cell renal cell carcinoma: analysis of VHL-dependent and VHL-independent pathways of tumorigenesis. Mol. Pathol., *53:* 137–144, 2000.
3. Martinez, A., Walker, R. A., Shaw, J. A., Dearing, S. J., Maher, E. R., and Latif, F. Chromosome 3p allele loss in early invasive breast cancer: detailed mapping and association with clinicopathological features. Mol. Pathol., *54:* 300–306, 2001.
4. Maitra, A., Wistuba, I. I., Washington, C., Virmani, A. K., Ashfaq, R., Milchgrub, S., Gazdar, A. F., and Minna, J. D. High-resolution chromosome 3p allelotyping of breast carcinomas and precursor lesions demonstrates frequent loss of heterozygosity and a discontinuous pattern of allele loss. Am. J. Pathol., *159:* 119–130, 2001.
5. Fullwood, P., Marchini, S., Rader, J. S., Martinez, A., Macartney, D., Broggini, M., Morelli, C., Barbanti-Brodano, G., Maher, E. R., and Latif, F. Detailed genetic and physical mapping of tumor suppressor loci on chromosome 3p in ovarian cancer. Cancer Res., *59:* 4662–4667, 1999.
6. Ejeskar, K., Aburatani, H., Abrahamsson, J., Kogner, P., and Martinsson, T. Loss of heterozygosity of 3p markers in neuroblastoma tumours implicate a tumour-suppressor locus distal to the *FHIT* gene. Br. J. Cancer, *77:* 1787–1791, 1998.
7. Wei, M. H., Latif, F., Bader, S., Kashuba, V., Chen, J. Y., Duh, F. M., Sekido, Y., Lee, C. C., Geil, L., Kuzmin, I., Zabarovsky, E., Klein, G., Zbar, B., Minna, J. D., and Lerman, M. I. Construction of a 600-kilobase cosmid clone contig and generation of a transcriptional map surrounding the lung cancer tumor suppressor gene (*TSG*) locus on human chromosome 3p21.3: progress toward the isolation of a lung cancer *TSG*. Cancer Res., *56:* 1487–1492, 1996.
8. Sekido, Y., Ahmadian, M., Wistuba, I. I., Latif, F., Bader, S., Wei, M. H., Duh, F. M., Gazdar, A. F., Lerman, M. I., and Minna, J. D. Cloning of a breast cancer homozygous deletion junction narrows the region of search for a 3p21.3 tumor suppressor gene. Oncogene, *16:* 3151–3157, 1998.
9. Lerman, M. I., and Minna, J. D. The 630-kb lung cancer homozygous deletion region on human chromosome 3p21.3: identification and evaluation of the resident candidate tumor suppressor genes. The International Lung Cancer Chromosome 3p21.3 Tumor Suppressor Gene Consortium. Cancer Res., *60:* 6116–6133, 2000.
10. Angeloni, D., Wei, M. H., Duh, F. M., Johnson, B. E., and Lerman, M. I. A G-to-A single nucleotide polymorphism in the human $\alpha 2\delta 2$ calcium channel subunit gene that maps at chromosome 3p21.3. Mol. Cell. Probes, *14:* 53–54, 2000.
11. Angeloni, D., Duh, F. M., Wei, M. F., Johnson, B. E., and Lerman, M. I. A G-to-A single nucleotide polymorphism in intron 2 of the human CACNA2D2 gene that maps at 3p21.3. Mol. Cell. Probes, *15:* 125–127, 2001.
12. Honorio, S., Gordon, K., MacCartney, D., Agathanggelou, A., and Latif, F. Identification of a single nucleotide polymorphism in the human $\alpha 2\delta 2$ calcium channel subunit gene. Mol. Cell. Probes, *15:* 391–393, 2001.
13. Dammann, R., Li, C., Yoon, J. H., Chin, P. L., Bates, S., and Pfeifer, G. P. Epigenetic inactivation of a RAS association domain family protein from the lung tumour suppressor locus 3p21.3. Nat. Genet., *25:* 315–319, 2000.
14. Agathanggelou, A., Honorio, S., Macartney, D. P., Martinez, A., Dallol, A., Rader, J., Fullwood, P., Chauhan, A., Walker, R., Shaw, J. A., Hosoe, S., Lerman, M. I., Minna, J. D., Maher, E. R., and Latif, F. Methylation-associated inactivation of RASSF1A from region 3p21.3 in lung, breast and ovarian tumours. Oncogene, *20:* 1509–1518, 2001.
15. Burbee, D. G., Forgacs, E., Zochbauer-Muller, S., Shivakumar, L., Fong, K., Gao, B., Randle, D., Kondo, M., Virmani, A., Bader, S., Sekido, Y., Latif, F., Milchgrub, S., Toyooka, S., Gazdar, A. F., Lerman, M. I., Zabarovsky, E., White, M., and Minna, J. D. Epigenetic inactivation of RASSF1A in lung and breast cancers and malignant phenotype suppression. J. Natl. Cancer Inst. (Bethesda), *93:* 691–699, 2001.
16. Astuti, D., Agathanggelou, A., Honorio, S., Dallol, A., Martinsson, T., Kogner, P., Cummins, C., Neumann, H. P., Voutilainen, R., Dahia, P., Eng, C., Maher, E. R., and Latif, F. RASSF1A promoter region CpG island hypermethylation in phaeochromocytomas and neuroblastoma tumours. Oncogene, *20:* 7573–7577, 2001.
17. Dammann, R., Yang, G., and Pfeifer, G. P. Hypermethylation of the cpG island of Ras association domain family 1A (RASSF1A), a putative tumor suppressor gene from the 3p21.3 locus, occurs in a large percentage of human breast cancers. Cancer Res., *61:* 3105–3109, 2001.
18. Morrissey, C., Martinez, A., Zatyka, M., Agathanggelou, A., Honorio, S., Astuti, D., Morgan, N. V., Moch, H., Richards, F. M., Kishida, T., Yao, M., Schraml, P., Latif, F., and Maher, E. R. Epigenetic inactivation of the *RASSF1A* 3p21.3 tumor suppressor gene in both clear cell and papillary renal cell carcinoma. Cancer Res., *61:* 7277–7281, 2001.
19. Byun, D. S., Lee, M. G., Chae, K. S., Ryu, B. G., and Chi, S. G. Frequent epigenetic inactivation of RASSF1A by aberrant promoter hypermethylation in human gastric adenocarcinoma. Cancer Res., *61:* 7034–7038, 2001.
20. Kwong, J., Lo, K. W., To, K. F., Teo, P. M., Johnson, P. J., and Huang, D. P. Promoter hypermethylation of multiple genes in nasopharyngeal carcinoma. Clin. Cancer Res., *8:* 131–137, 2002.
21. Kuzmin, I., Gillespie, J. W., Protopopov, A., Geil, L., Dreijerink, K., Yang, Y., Vocke, C. D., Duh, F. M., Zabarovsky, E., Minna, J. D., Rhim, J. S., Emmert-Buck, M. R., Linehan, W. M., and Lerman, M. I. The *RASSF1A* tumor suppressor gene is inactivated in prostate tumors and suppresses growth of prostate carcinoma cells. Cancer Res., *62:* 3498–3502, 2002.
22. Honorio, S., Agathanggelou, A., Wernert, N., Rothe, M., Maher, E. R., and Latif, F. Frequent epigenetic inactivation of the *RASSF1A* tumour suppressor gene in testicular tumours and distinct methylation profiles of seminoma and nonseminoma testicular germ cell tumours. Oncogene, *22:* 461–466, 2003.
23. Vos, M. D., Ellis, C. A., Bell, A., Birrer, M. J., and Clark, G. J. Ras uses the novel tumor suppressor RASSF1 as an effector to mediate apoptosis. J. Biol. Chem., *275:* 35669–35672, 2000.
24. Ortiz-Vega, S., Khokhlatchev, A., Nedwidek, M., Zhang, X. F., Dammann, R., Pfeifer, G. P., and Avruch, J. The putative tumor suppressor RASSF1A homodimerizes and heterodimerizes with the Ras-GTP binding protein Nore1. Oncogene, *21:* 1381–1390, 2002.
25. Vavvas, D., Li, X., Avruch, J., and Zhang, X. F. Identification of Nore1 as a potential Ras effector. J. Biol. Chem., *273:* 5439–5442, 1998.
26. Khokhlatchev, A., Rabizadeh, S., Xavier, R., Nedwidek, M., Chen, T., Zhang, X. F., Seed, B., and Avruch, J. Identification of a novel Ras-regulated proapoptotic pathway. Curr. Biol., *12:* 253–265, 2002.
27. van Engeland, M., Roemen, G. M., Brink, M., Pachen, M. M., Weijenberg, M. P., de Bruine, A. P., Arends, J. W., van den Brandt, P. A., de Goeij, A. F., and Herman, J. G. K-ras mutations and RASSF1A promoter methylation in colorectal cancer. Oncogene, *21:* 3792–3795, 2002.
28. Shivakumar, L., Minna, J., Sakamaki, T., Pestell, R., and White, M. A. The RASSF1A tumor suppressor blocks cell cycle progression and inhibits cyclin D1 accumulation. Mol. Cell. Biol., *22:* 4309–4318, 2002.
29. Ross, D. T., Scherf, U., Eisen, M. B., Perou, C. M., Rees, C., Spellman, P., Iyer, V., Jeffrey, S. S., Van de Rijn, M., Waltham, M., Pergamenschikov, A., Lee, J. C., Lashkari, D., Shalon, D., Myers, T. G., Weinstein, J. N., Botstein, D., and Brown, P. O. Systematic variation in gene expression patterns in human cancer cell lines. Nat. Genet., *24:* 227–235, 2000.
30. Birchmeier, W., and Behrens, J. Cadherin expression in carcinomas: role in the formation of cell junctions and the prevention of invasiveness. Biochim. Biophys. Acta, *1198:* 11–26, 1994.
31. Takeichi, M. Cadherins in cancer: implications for invasion and metastasis. Curr. Opin. Cell Biol., *5:* 806–811, 1993.
32. Bremnes, R. M., Veve, R., Hirsch, F. R., and Franklin, W. A. The E-cadherin cell-cell adhesion complex and lung cancer invasion, metastasis, and prognosis. Lung Cancer, *36:* 115–124, 2002.
33. Reyes-Mugica, M., Meyerhardt, J. A., Rzasa, J., Rimm, D. L., Johnson, K. R., Wheelock, M. J., and Reale, M. A. Truncated DCC reduces *N*-cadherin/catenin expression and calcium-dependent cell adhesion in neuroblastoma cells. Lab Invest ig., *81:* 201–210, 2001.
34. Prasad, G. L., Fuldner, R. A., and Cooper, H. L. Expression of transduced tropomyosin 1 cDNA suppresses neoplastic growth of cells transformed by the *ras* oncogene. Proc. Natl. Acad. Sci. USA, *90:* 7039–7043, 1993.
35. Hirota, T., Morisaki, T., Nishiyama, Y., Marumoto, T., Tada, K., Hara, T., Masuko, N., Inagaki, M., Hatakeyama, K., and Saya, H. Zyxin, a regulator of actin filament assembly, targets the mitotic apparatus by interacting with h-warts/LATS1 tumor suppressor. J. Cell Biol., *149:* 1073–1086, 2000.
36. Dilakyan, E. A., Zhurbitskaya, V. A., Vinokurova, S. V., Gureeva, T. A., Lubkova, O. N., Topol, L. Z., Kisseljov, F. L., and Solovyeva, N. I. Expression of cathepsin L and its endogenous inhibitors in immortal and transformed fibroblasts. Clin. Chim. Acta., *309:* 37–43, 2001.
37. Premzl, A., Puizdar, V., Zavasnik-Bergant, V., Kopitar-Jerala, N., Lah, T. T., Katunuma, N., Sloane, B. F., Turk, V., and Kos, J. Invasion of ras-transformed breast epithelial cells depends on the proteolytic activity of cysteine and aspartic proteinases. Biol. Chem., *382:* 853–857, 2001.
38. Dhanesuan, N., Sharp, J. A., Blick, T., Price, J. T., and Thompson, E. W. Doxycycline-inducible expression of SPARC/Osteonectin/BM40 in MDA-MB-231 human breast cancer cells results in growth inhibition. Breast Cancer Res. Treat., *75:* 73–85, 2002.
39. Chlenski, A., Liu, S., Crawford, S. E., Volpert, O. V., DeVries, G. H., Evangelista, A., Yang, Q., Salwen, H. R., Farrer, R., Bray, J., and Cohn, S. L. SPARC is a key Schwannian-derived inhibitor controlling neuroblastoma tumor angiogenesis. Cancer Res., *62:* 7357–7363, 2002.
40. Wasylyk, B., Hagman, J., and Gutierrez-Hartmann, A. Ets transcription factors: nuclear effectors of the Ras-MAP-kinase signalling pathway. Trends Biochem. Sci., *23:* 213–216, 1998.
41. Foos, G., Garcia-Ramirez, J. J., Galang, C. K., and Hauser, C. A. Elevated expression of Ets2 or distinct portions of Ets2 can reverse Ras-mediated cellular transformation. J. Biol. Chem., *273:* 18871–18880, 1998.
42. Paz, M. F., Fraga, M. F., Avila, S., Guo, M., Pollan, M., Herman, J. G., and Esteller, M. A systematic profile of DNA methylation in human cancer cell lines. Cancer Res., *63:* 1114–1121, 2003.
43. Autuori, F., Farrace, M. G., Oliverio, S., Piredda, L., and Piacentini, M. "Tissue" transglutaminase and apoptosis. Adv. Biochem. Eng. Biotechnol., *62:* 129–136, 1998.
44. Chen, S., Lin, F., Iismaa, S., Lee, K. N., Birckbichler, P. J., and Graham, R. M. α1-Adrenergic receptor signaling via Gh is subtype specific and independent of its transglutaminase activity. J. Biol. Chem., *271:* 32385–32391, 1996.
45. Upchurch, H. F., Conway, E., Patterson MK Jr., and Maxwell, M. D. Localization of cellular transglutaminase on the extracellular matrix after wounding: characteristics of the matrix bound enzyme. J. Cell Physiol., *149:* 375–382, 1991.
46. Gentile, V., Thomazy, V., Piacentini, M., Fesus, L., and Davies, P. J. Expression of tissue transglutaminase in Balb-C 3T3 fibroblasts: effects on cellular morphology and adhesion. J. Cell Biol., *119:* 463–474, 1992.
47. Nakaoka, H., Perez, D. M., Baek, K. J., Das, T., Husain, A., Misono, K., Im, M. J., and Graham, R. M. Gh: a GTP-binding protein with transglutaminase activity and receptor signaling function. Science (Wash. DC), *264:* 1593–1596, 1994.
48. Gal, S., and Gottesman, M. M. The major excreted protein of transformed fibroblasts is an activable acid-protease. J. Biol. Chem., *261:* 1760–1765, 1986.